

A Journal of the German Chemical Society

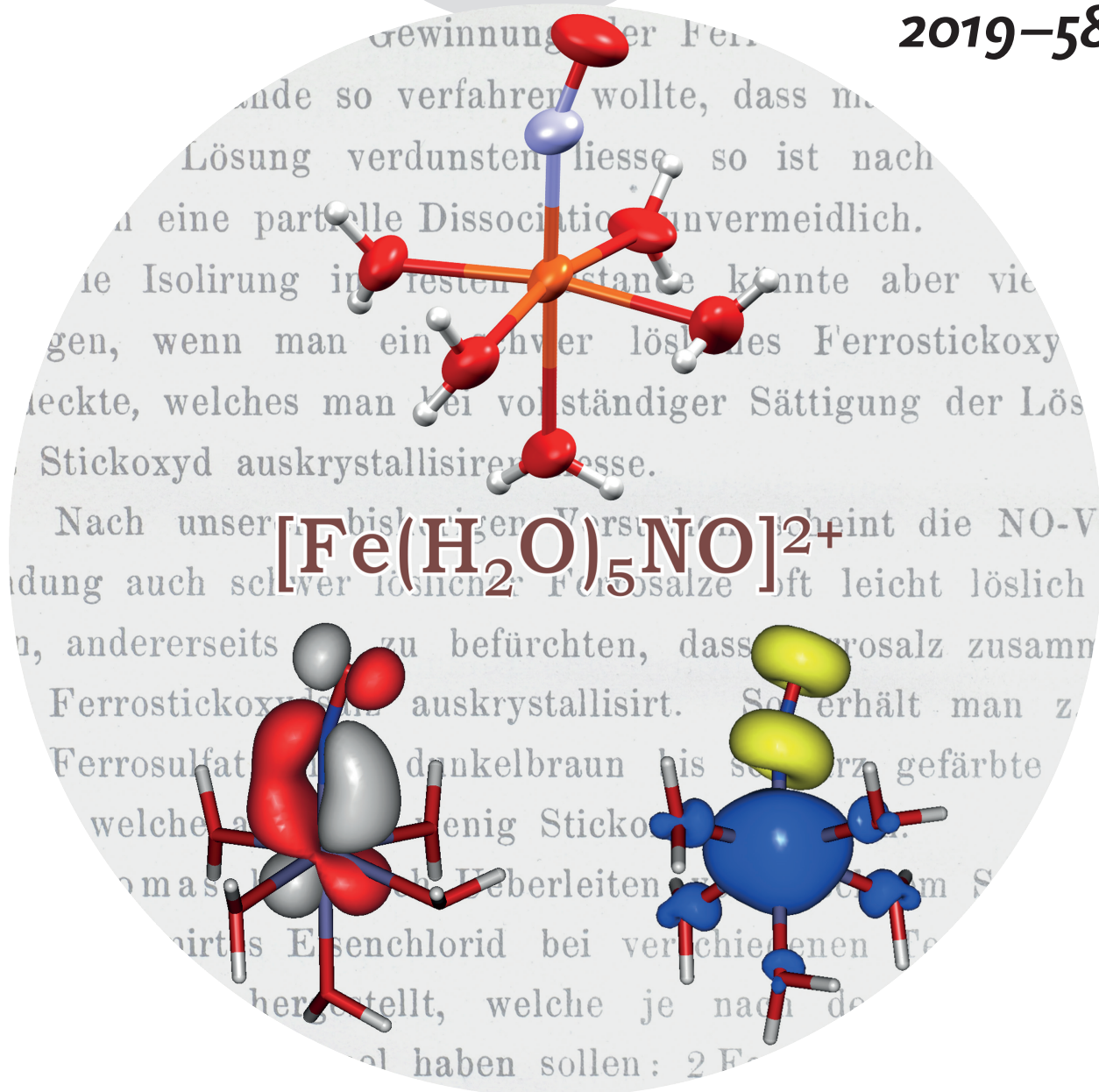
Angewandte Chemie

GDCh

International Edition

www.angewandte.org

2019–58/25



Cover Picture

P. Klüfers and G. Monsch

$[\text{Fe}(\text{H}_2\text{O})_5(\text{NO})]^{2+}$, the "Brown-Ring" Chromophore

Coordination Chemistry

International Edition: DOI: 10.1002/anie.201902374

German Edition: DOI: 10.1002/ange.201902374

[Fe(H₂O)₅(NO)]²⁺, the “Brown-Ring” Chromophore

Georg Monsch and Peter Klüfers*

Abstract: Although the “brown-ring” ion, [Fe(H₂O)₅(NO)]²⁺ (**1**), has been a research target for more than a century, this poorly stable species had never been isolated. We now report on the synthesis of crystals of a salt of **1** which allowed us to tackle the unique bonding situation on an experimental basis. As a result of the bonding analysis, two stretched, spin-polarised π -interactions provide the Fe–NO binding—and challenge the concept of “oxidation state”.

The investigation of the [Fe(H₂O)₅(NO)]²⁺ (**1**) ion, the coloured component of the “brown ring” of the analytical nitrate test (Figure 1), has been an enduring issue in inorganic

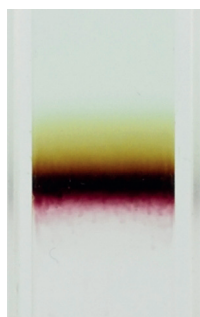


Figure 1. The so-called “brown ring” which forms between the bottom layer of concentrated sulfuric acid and the top layer that contains ferrous sulfate and nitrate. The colour stems from {FeNO}⁷ species that form after the reduction of nitrate ($3\text{Fe}^{2+} + \text{NO}_3^- + 4\text{H}^+ \rightarrow 3\text{Fe}^{3+} + \text{NO} + 2\text{H}_2\text{O}$) from NO and excess Fe²⁺.

chemistry. A known chromophore since the 19th century, the first period of intensive research on this ion dates back to the first decade of the 20th century, where the competing groups of Manchot and Kohlschütter demonstrated the cationic nature of **1** as well as the equimolar amount of iron and nitric oxide in this species, which they obtained by the reaction of ferrous salts and nitric oxide gas in acidic aqueous solution.^[1] The current, generally accepted formula was deduced by Wilkinson et al. in 1958; moreover, the $S=3/2$ spin of the species was reported in that publication as well. From the latter value and the IR absorption around 1800 cm⁻¹, the authors deduced **1** to be an iron(I) complex with an NO⁺ ligand.^[2] This interpretation persisted until the re-interpretation given in 2002 by Stochel, van Eldik, and others who

favoured **1** comprising a high-spin, $S=5/2$, iron(III) central atom antiferromagnetically coupled to a triplet NO⁻ ligand.^[3] Thus, the former [Fe^I(H₂O)₅(NO⁺)]²⁺ formulation was rewritten as [Fe^{III}(H₂O)₅(³NO⁻)]²⁺. Two years later, that re-assignment was questioned by Cheng et al. who, in a DFT approach, proposed that the formula [Fe^{II}(H₂O)₅(NO⁰)]²⁺ was more appropriate. In the same work, they stressed the linearity of the Fe–N–O moiety in **1**'s ground state.^[4] In 2010, the Ghosh group also reported a linear FeNO entity and alluded to the unusually flat bending potential of the triatomic group.^[5] Wavefunction theory (WFT), as applied by Radón et al. in the same year, directed attention to the significance of nondynamic correlation within the Fe–NO π -bonds.^[6] More recent analyses of Fe–NO bonding include the negligible charge transfer between a dicationic Fe atom and the neutral NO reactant.^[7] The continuing interest of theoretical groups in **1** is, of course, not only maintained because it is taught to undergraduates in analytical courses. In fact, **1** is the parent compound of a family of species of current biochemical interest, the quartet {FeNO}⁷ species (the superscript in this “Enemark–Feltham” notation is the sum of the metal d and the NO π^* electrons). We refer to the literature for the bioinorganic issue in the Supporting Information. Further {FeNO}⁷ ($S=3/2$) species closely related to **1** had been discovered more than a century ago when the experimental conditions of the brown-ring test were varied. Thus, in concentrated hydrochloric acid, the reaction of ferrous chloride with nitric oxide yields the green [FeCl₃(NO)]⁻ chromophore.^[8] Herein, we report on the isolation and investigation of the “brown-ring” chromophore itself including an analysis of the bonding situation based on the now available experimental structural data.

Species **1** is an easily decomposable coordination entity. The first systematic investigation by Manchot already unravelled its limited stability in terms of NO loss in aqueous solution. Prepared from a ferrous salt and NO gas in water, **1** rapidly releases NO when inert gas is passed through the solution. Accordingly, for their kinetic investigation in aqueous solution, the van Eldik group made use of the fact that **1** is rapidly photolysed by visible light of, apparently, any wavelength. In their survey of more than 100 quartet {FeNO}⁷ complexes, the parent aqua species **1** has the lowest stability of all.^[9] Thus, not unexpectedly, the isolation of chocolate-brown, large crystals (see a photo in Ref. [1f]) of the claimed formula 2FeSO₄·NO·13H₂O by Manchot has been questioned by researchers who had attempted to repeat the synthesis (Wilkinson, 1958: “rather ill-defined solids”).^[1f,2] In fact, in our own attempts, we reproduced Manchot's deep-brown crystals. However, all batches proved to be FeSO₄·7H₂O = [Fe(H₂O)₆](SO₄)·H₂O with small amounts (max. 14%) of NO on one of the point positions of the aqua ligands (see the Supporting Information for details).

[*] M. Sc. G. Monsch, Prof. Dr. P. Klüfers
Department Chemie der Ludwig-Maximilians-Universität
Butenandtstrasse 5–13, 81377 München (Germany)
E-mail: kluef@cup.uni-muenchen.de

Supporting information and the ORCID identification numbers for the authors of this article can be found under:
<https://doi.org/10.1002/anie.201902374>.

Although attempts to isolate salts of the brown chromophore with simple anions were unsuccessful, we have now isolated **1** as the cation in brown crystals of the general formula $[\text{Fe}(\text{H}_2\text{O})_5(\text{NO})][\text{M}^{\text{III}}(\text{fpin})_2(\text{H}_2\text{O})_2 \cdot x\text{H}_2\text{O}]$ ($\text{M} = \text{Fe}, \text{Ga}$; $x \approx 8.3$). The dianionic ligand fpin is the bidentate perfluoropinacolato- $\kappa^2\text{O}, \text{O}'$ chelator which we and others have used to prepare tetracoordinate, more or less planar, high-spin ferrates(II) with the $[\text{Fe}(\text{fpin})_2]^{2-}$ anion.^[10] Solutions containing this latter anion absorbed NO to yield the five-coordinate $[\text{Fe}(\text{fpin})_2(\text{NO})]^{2-}$ ion.^[11] In contrast, aqueous reaction mixtures with an equimolar ratio of Fe and fpin reacted under precipitation of crystalline **1** $[\text{Fe}^{\text{III}}(\text{fpin})_2(\text{H}_2\text{O})_2 \cdot x\text{H}_2\text{O}]$. Iron(III) formation occurred with the liberation of N_2O which was detected in the gas phase by means of its IR signature. In order to investigate **1** without the potentially interfering ferrate(III), we modified the preparation by using gallium as the anion's central atom in the overall acidic solution. The brown crystals of **1** $[\text{M}^{\text{III}}(\text{fpin})_2(\text{H}_2\text{O})_2 \cdot x\text{H}_2\text{O}]$ were suitable for X-ray work for both anions (with the gallate anion being iron-free in terms of X-ray data). The structure of **1** in the gallate crystals is shown in Figure 2.

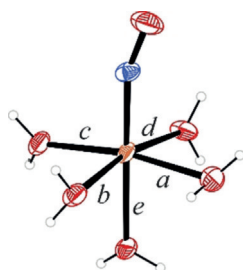


Figure 2. The molecular structure of **1** in crystals of the gallate (50% probability ellipsoids).^[12] For a – e and other distances and angles see Table S1 in the Supporting Information.

The structure analysis showed that, as suggested by Wilkinson, the brown chromophore of the solids in fact is the pentaquanitrosyliron(2+) ion.^[2] However, the C_1 symmetry of **1** as well as distances and angles are at variance with the theoretical predictions (see the Supporting Information for an overview). In particular, the claimed linearity of the Fe–N–O unit is not observed in either of the salts (161° in the gallate, 162° in the ferrate). However, in a computational approach on the BP86/def2-TZVP level of theory, we succeeded in coming to a closer match between calculated and measured data (including the Fe–N–O angle) by taking the experimentally determined conformation of the pentaqua ion as the starting point (for details see the Supporting Information).

On the basis of the now available structural data, we first tackled the issue of the unusual extent of nondynamical correlation within the nitrosyl–metal moiety, the computational trace of hindered orbital overlap. As a convenient DFT-based tool we used the fractional-occupation-number-weighted-density (FOD) approach recently introduced by Grimme.^[13] Figure 3 shows the so-called “hot” electrons that deserve a correlated treatment. A comparison of **1** with related species shows that, as a rule, the two π -interactions

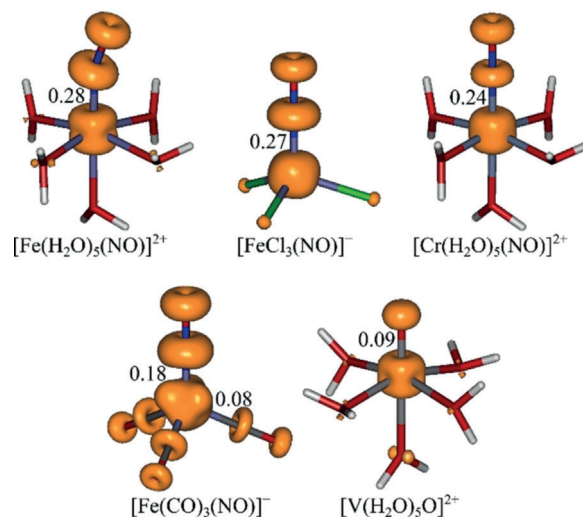


Figure 3. FOD plots (BHLYP, $T = 15\,000$ K, isovalue 0.005 a.u.) indicating the “hot”, nondynamically correlated electrons. Numbers close to the metal–ligand bonds give the antibond population in CASSCF(n,m) approaches: (9,13) for **1** and $[\text{FeCl}_3(\text{NO})]^-$, (7,8) for the Cr species, (14,14) for the carbonyl complex, and (7,8) for the vanadyl ion. The latter ion shows a σ -antibond occupation of 0.07 in addition to π -correlation within the $\text{V}=\text{O}$ fragment; hence, the typical “ π -donor” appears filled here. The occupation pattern of the carbonyl complex roughly resembles published data for smaller active spaces (4,4 and 10,10).^[14]

between the nitrosyl ligand and the respective metal orbitals suffer from hindered overlap. Hence, in a multiconfigurational treatment (see below), the M–NO π -bonds are depopulated and their antibonds are populated accordingly. The occupation of each π -M–NO antibond for closely related complexes of divalent central metals after their reaction with NO is given in the top row of Figure 3. The bottom row of the figure stresses the similarity to further species: the diamagnetic $\{\text{FeNO}\}^{10}$ anion $[\text{Fe}(\text{CO})_3(\text{NO})]^-$ with a low-valent central atom also shows the maximum stretch for the Fe–NO interaction, accompanied by a minor effect on the weaker π -accepting CO ligands.^[14] The Fe–NO antibond population of this species resembles that of low-spin- $\{\text{RuNO}\}^6$ entities.^[15] The latter fact shows that we are obviously dealing with a general property of nitrosyl complexes. In comparison, a double π -donor such as the terminal oxido ligand in $[\text{V}(\text{H}_2\text{O})_5\text{O}]^{2+}$ shows a significantly lower antibond population.

The result of a correlated analysis by means of CASSCF approaches using various active spaces is depicted in Figure 4. Due to the marked Fe–NO π -antibonding contributions, the leading configuration (arrows in Figure 4) contributes 62% only to the species's ground state, indicating a significant stretch of the π -Fe–NO interactions. As the physical origin of this stretch, we see multiple instances of Pauli repulsion in the nitrosyl species in question:

- First, as elucidated by Kaupp, the absence of radial nodes in the 3d orbitals causes significant overlap density with the occupied 3s and 3p orbitals.^[16] As the σ/π antibond population of the vanadyl ion (Figure 3) shows, 3d–M–L Pauli repulsion is more pronounced for π -type bonds,

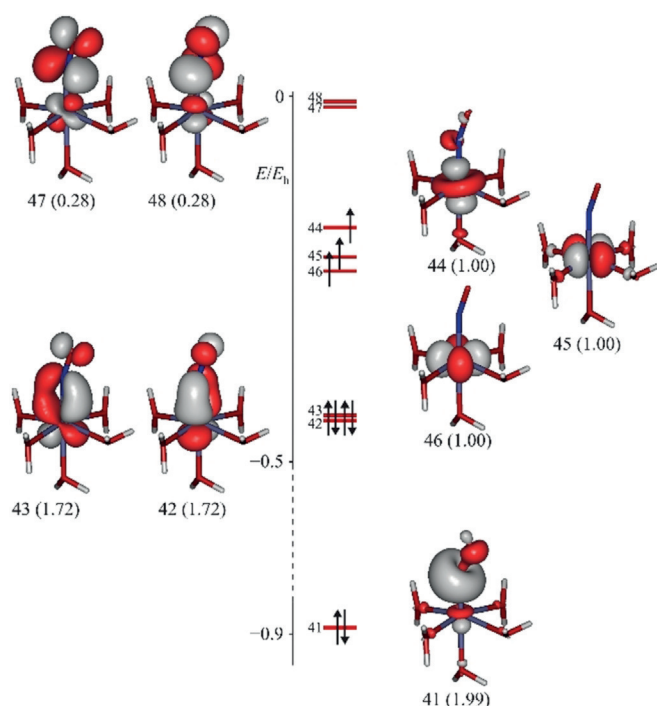


Figure 4. Frontier orbitals of the $[\text{Fe}(\text{H}_2\text{O})_5(\text{NO})]^{2+}$ ion [CASSCF(9,13)/def2-TZVP; isovalue 0.06 a.u.]. Orbital numbering and occupation (in parentheses). The 22211100 occupation pattern indicated by the arrows refers to the ground state's leading configuration (62% contribution).

which need closer internuclear distances for optimum overlap.

- Over and above this common factor, there is a still more significant contribution to the Pauli repulsion scenario that makes NO unique. Taking an NO^+ ion as a starting point, covalent bonding to the nitrosyl moiety relies on the population of the NO^+ LUMOs, the two degenerate N–O π^* MOs. The overlap of suitable metal orbitals and these NO ligand orbitals is, thus, always encumbered by Pauli repulsion between the M–NO bond and the two N–O bonding π -pairs, which occupy almost the same spatial region as their antibonding counterparts.
- Lastly, there is a special aspect of quartet $[\text{FeNO}]^7$ species, namely the obviously repulsive Fe- d_{z^2} -NO σ -contact which appears alleviated by Fe-N-O bending. Figure 4 shows bond (MO 41) and antibond (MO 44) of this interaction. An occupied antibond is missing in the chromium analogue. As a result, the M–NO bond length in $[\text{Cr}(\text{H}_2\text{O})_5(\text{NO})]^{2+}$ is ca. 0.1 Å shorter than that in **1** (1.697 vs. 1.786 Å). Moreover, the Cr-N-O angle is close to 180°.

The spin population of **1** and related species as depicted in Figure 5 follows the rules compiled in Refs. [17] and [18]. Hence, major-spin delocalisation into ligand orbitals is found for the nonorthogonal interaction of an electron-pair donor and a singly occupied metal orbital. For **1**, both the σ - and π -interactions of the aqua ligands and the Fe- d_{xy} , Fe- $d_{x^2-y^2}$ and Fe- d_{z^2} orbitals show this behaviour. The same holds for the chloride orbitals in the related $[\text{FeCl}_3(\text{NO})]^-$, and the π -interactions of the aqua ligands with the M- d_{xy} orbitals in the

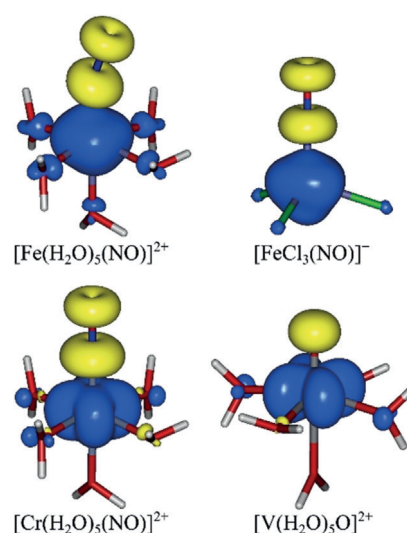


Figure 5. The spin population in some species with dominant M–L π -bonding (BP86/def2-TZVP; positive spin values blue, negative values yellow; isovalues in a.u.: 0.1 for the top-row species, 0.05 for the bottom-row dications).

bottom-row species of Figure 5. Spin polarisation is experienced by electron pairs on orthogonal interaction with the major spin. Hence, both Fe–NO π -interactions accumulate α -spin density at the metal centre and thus leave β -spin density on the ligand. The same holds for the σ -interactions of the aqua ligands and the empty M- $d_{x^2-y^2}$ orbitals in the Cr and V species as well as the σ/π components of the $\text{V}=\text{O}$ bond. The extent of the spin delocalisation or polarisation mirrors the respective orbital overlap. Notably, none of the potential M–NO σ -bonds give rise to a considerable amount of the expected α -spin delocalisation on the ligand side for the isovalues specified in the caption of Figure 5 (note the faint spin delocalisation in the NO ligand's σ -part for the Fe and the Cr species at a lower isovalue in Figure S2).

Numerical values obtained for the spin population of the nitrosyl ligand confirm published analyses by resulting in the, at least, moderate agreement of WFT and nonhybrid-DFT values.^[6] For various active spaces (n,m), the CASSCF values were -0.64 (7,7), -0.54 (7,12), -0.51 (9,13), whereas pure density functionals revealed -0.68 (BP86), -0.82 (OLYP), -0.84 (OPBE) and -0.71 (TPSS; all calculations with the def2-TZVP basis set). Hybrid functionals accumulate more minority-spin density on the nitrosyl ligand—the higher the HF percentage (in parentheses), the higher the spin polarisation: TPSSH (10%) -0.91 , B3LYP (20%) -1.00 , BHLYP (50%) -1.28 ; ω B97M-V (var.) -1.05 . Ref. [6] sees the higher values for the NO's β -spin occupation as an unphysical “overpolarisation” (for another in-depth study on the overestimation of spin polarisation in related $[\text{FeNO}]^7$ species see Ref. [19]). A merely technical detail at first glance, this issue will, however, deserve attention on attempts to assign oxidation states.

Published oxidation-state (OS) assignments for **1** ranging from $\text{Fe}^{\text{I}}(\text{NO}^+)$ to $\text{Fe}^{\text{III}}(\text{NO}^-)$ mirror the uncertainty about how to distribute the electrons of the π -bonds. Hence, the oldest assignments, which treat the nitrosyl ligand as an NO^+

cation, look at the π -bonds as metal-associated backbonds. In fact, the attempt to determine OSs in **1** becomes a challenge to the concept of “oxidation state” itself. A look at charges may serve as a starting point. On the application of the various partitioning methods, a more or less neutral nitrosyl ligand is obtained without noteworthy differences among the methods. In detail, the NO moiety carries the following charge, depending on the given procedure: -0.10 (QTAIM), $+0.09$ (NPA), $+0.19$ (ECDA), -0.05 (IAO/IBO), $+0.18$ (Mulliken), all from BP86/def2-TZVP data, $+0.06$ (Mulliken) from CASSCF(9,13) data. At first glance, the most recently published $\text{Fe}^{\text{II}}(\text{NO}^0)$ formulation thus appears in line with those calculations.^[4] In fact, there was a tendency in the past to interpret oxidation states as “real” charges. A statement from a 2010 work in fact stresses the term “real oxidation number”: “the $\text{Fe}^{\text{I}} \text{NO}^+$ description should merely be regarded as a formal one. In reality, the extremely strong $d \rightarrow \pi^*$ backdonation repopulates the ‘empty’ NO π^* orbitals and changes the real oxidation number of Fe to between II and III”.^[6]

However, in 2016, the IUPAC strengthened the OS’s original definition as a winner-takes-all principle by founding the OS on the ionic approximation (IA) of heteronuclear bonds. Various tools may support the IA, among them the inspection of the share of an atom’s AO in the bonding MO.^[20] Ignoring the spin population renders the IA for **1** a straightforward task. Fe–NO bonding relies on the two (stretched) π -bonds (MOs 42 and 43 in Figure 4). In terms of orbital coefficients, they are mainly metal-centered; hence, the IA allocates the two π -pairs to the metal. Thus, with the seven electrons in favour of the metal and the empty π^* N–O MOs of the ligand, the IA results in the classic $\text{Fe}^{\text{I}}(\text{NO}^+)$ formulation, or, equivalently, d^7 , due to the relationship $\text{OS} = N - n$ with N as the transition-metal’s group number.^[20]

This apparently clear situation becomes complicated only after the spin population is taken into account. Notably, computational algorithms which extract the d^n configuration of the central atom from the wavefunction, treat the α - and β -regimes of a paramagnetic species separately to end up with n as the sum of n_α and n_β . Among the various methods such as Sit’s approach, including its NBO-based variant, Head-Gordon’s LOBA method and Salvador’s recent EOS approach, the latter method appears particularly robust to adequately treat a scenario that is governed by spin-polarised (back)bonds.^[21] To prepare us for the evaluation of the results, we should take one more look at the ligand’s “real” zero charge beforehand. For this, one of the four π -electrons has to be shifted to an NO^+ core, which resembles a $1/2$ ligand-allocated electron per π -bond. Leaving the majority of three electrons at the metal, we formulated M \rightarrow L backbonds above. In contrast, at complete spin polarisation (the B3LYP case above), one of two β -spins has to be shifted to the NO^+ core to end at the NO^0 moiety. For the resulting equal distribution of the β -spin among the metal and the ligand in the sense of a “ β -covalency”, the OS assignment is much more borderline. In other words, the above-mentioned overpolarisation makes the correct allocation of the β -spin highly method-dependent. To be specific, the EOS approach remains with the $\text{Fe}^{\text{I}}(\text{NO}^+)$ partitioning when applied on

top of the three methods with the lowest spin polarisation, namely the WFT method CASSCF(7,12), the GGA-functional BP86 and the *meta*-GGA-functional TPSS. The higher β -spin accumulation of the remaining functionals—specifically pronounced for the hybrid functionals with a larger HF percentage—yield the $\text{Fe}^{\text{III}}(\text{NO}^-)$ formulation.^[22] Hence, **1** comes up with two challenges for the OS concept vocabulary. First, the strong acceptor ligand probes the proper treatment of backbonds. Second, for the paramagnetic species **1** it does so mainly in the β -channels of the two π -interactions. The first issue is imperfectly covered by the IUPAC recommendation (which does not pay much attention to backbonds: CO is treated as a simple donor ligand in the examples). The second issue is not covered at all. Although the practice in computational approaches, α/β -separation in spin-polarised bonds is incompatible with the allocation of electron *pairs* in the framework of the IA approach.

What about Mößbauer data which are often considered relevant in a discussion on oxidation states? Isomer shift and quadrupole splitting of **1** (zero-field ^{57}Fe Mößbauer data of the ferrate of **1**; $T = 133$ K, isomer shift: $\delta = 0.655(3)$ mm s^{-1} , quadrupole splitting: $|\Delta E_Q| = 2.031(8)$ mm s^{-1} , Figure S4) agree with published data on frozen aqueous solutions where **1** was found as a minor species in equilibrium with hexaquaairon(II).^[3] In the publications cited above, the isomer shift is frequently seen as a confirmation of the assigned OS. However, Ref. [23] points out that the isomer shift, which is proportional to the electron contact density at the Fe nucleus, depends on several parameters: the charge of the species, its spin and the covalency of the bonds. Hence, for the unique bonding situation in the $\{\text{FeNO}\}^7(S = 3/2)$ species, the isomer shift simply is what it is, and a straightforward decision about the OS cannot be made. However, the congruence of the measured and calculated parameters can be evaluated. Thus, for **1**, isomer shift and quadrupole splitting were well reproduced on the TPSSh level of theory [basis sets: CP(PPP) for Fe, def2-TZVP for all other atoms; $\delta = 0.652$ mm s^{-1} , $|\Delta E_Q| = 2.188$ mm s^{-1}].

In conclusion, we may return to the issue that is responsible for viewing **1** as an iconic object of inorganic chemistry. **1** is the rare example of a species that is relevant for both undergraduate teaching and current research. Thus, let us try to teach a somewhat advanced undergraduate student the results of this investigation. To attune one to the most characteristic peculiarity of the NO moiety, we may start with the properties of nitric oxide at very low temperatures. In the most recent report, aggregates such as the dimer, the trimer and the tetramer were detected in helium droplets, with the trapeziform *cis*-dimer N_2O_2 as the most stable species.^[24] With an N \cdots N distance of about 2.3 Å and a bond dissociation energy D_0 of 8–10 kJ mol^{-1} , an unusually weak bond is formed by the obviously hindered overlap of the singly occupied π^* MOs of the two NO molecules (Figure S3 in the Supporting Information shows a sketch of such repulsive π/π^* interactions.) One step closer to the formal NO^+ ligand are salts such as nitrosyl hydrogensulfate, the “lead-chamber” crystals. The student may argue that, with the moderate electronegativity difference $\chi_{\text{O}} - \chi_{\text{N}}$, polar covalent bonds such as $\text{O}=\text{N}^{\delta+}-\text{O}^{\delta-}-\text{SO}_3\text{H}$ would prevail in such a compound. In fact, the bond is

largely ionic according to $\text{HOSO}_3^- \text{NO}^+$, the electronegativities of neighbouring atoms be as they may.^[25] Again, the enhanced Pauli repulsion caused by the two π pairs of the cation appears to be the reason for the lower-than-expected tendency of NO^+ to fill its π^* MOs with the electron density of an approaching nucleophile.

Keeping in mind this peculiarity of the Lewis acid NO^+ , a high-spin $[\text{Fe}^{\text{I}}(\text{H}_2\text{O})_5]^+$ entity as the Lewis base will donate some electron density to the ligand. However, due to the considerable metal character of the formed Fe–NO π -bonds, the metal is not oxidised, but simply metal-centered backbonds are established. Due to the largely nonbonding/repulsive situation within the Fe- d_{z^2} -NO(3σ)² couple, these backbonds are more or less solely responsible for the limited stability of the aquated $\{\text{FeNO}\}^7$ entity. Thus, **1** is part of a series: the bonds are weakened by incomplete overlap due to marked Pauli repulsion as are the bonding situations in “ N_2O_2 ” or $\text{NO}(\text{HSO}_4)$. Regarding the assignment of an OS or, likewise, the d^n configuration of the iron atom, an instructor may decide to abstain from teaching OSs just on the basis of **1**, or, likewise, to demonstrate either the limits of a formal concept or to discuss sensible future extensions of the OS idea—the latter with the aim to include the current computational progress.^[21c] Meanwhile, there are no mandatory reasons to deprecate the $\text{Fe}^{\text{I}}(\text{NO}^+)$ formula in favour of the $\text{Fe}^{\text{II}}(\text{NO}^0)$ or the $\text{Fe}^{\text{III}}(\text{NO}^-)$ formulation.

The physical origin of the brown colour of **1** can be traced back to two types of electronic transitions, mostly from the Fe–NO π -bond MOs to the singly occupied, metal-based MOs of Figure 4, as well as to the Fe–NO π^* -antibonds. Details will be published separately.

Acknowledgements

We are indebted to Profs. Fritz Wagner (TU München), and Felix Tuzcek (CAU Kiel) for the Mößbauer measurements and their interpretation, as well as to Dr. Pedro Salvador (Univ. de Girona) for the calculation of the EOSs for the various computational methods and for helpful discussions. We gratefully acknowledge financial support from the DFG priority program SPP1740 (KL 624/18-1), aimed at “Reactive bubbly flows”.

Conflict of interest

The authors declare no conflict of interest.

Keywords: ab initio calculations · coordination chemistry · donor–acceptor systems · iron complexes · nitrosyls · oxidation states

How to cite: *Angew. Chem. Int. Ed.* **2019**, *58*, 8566–8571
Angew. Chem. **2019**, *131*, 8654–8659

[1] a) V. Kohlschütter, P. Sazanoff, *Ber. Dtsch. Chem. Ges.* **1911**, *44*, 1423–1432; b) V. Kohlschütter, M. Kutscheroff, *Ber. Dtsch. Chem. Ges.* **1907**, *40*, 873–878; c) V. Kohlschütter, M. Kutscher-

off, *Ber. Dtsch. Chem. Ges.* **1904**, *37*, 3044–3052; d) W. Manchot, K. Zechentmayer, *Justus Liebigs Ann. Chem.* **1906**, *350*, 368–389; e) W. Manchot, *Ber. Dtsch. Chem. Ges.* **1914**, *47*, 1601–1614; f) W. Manchot, F. Huttner, *Justus Liebigs Ann. Chem.* **1910**, *372*, 153–178; g) W. Manchot, *Ber. Dtsch. Chem. Ges.* **1914**, *47*, 1614–1616.

- [2] W. P. Griffith, J. Lewis, G. Wilkinson, *J. Chem. Soc.* **1958**, 3993–3998.
- [3] A. Wanat, T. Schnepfensieper, G. Stochel, R. van Eldik, E. Bill, K. Wieghardt, *Inorg. Chem.* **2002**, *41*, 4–10.
- [4] H.-Y. Cheng, S. Chang, P.-Y. Tsai, *J. Phys. Chem. A* **2004**, *108*, 358–361.
- [5] J. Conradie, K. H. Hopmann, A. Ghosh, *J. Phys. Chem. B* **2010**, *114*, 8517–8524.
- [6] M. Radoń, E. Broclawik, K. Pierloot, *J. Phys. Chem. B* **2010**, *114*, 1518–1528.
- [7] a) E. Broclawik, A. Stępniewski, M. Radoń, *J. Inorg. Biochem.* **2014**, *136*, 147–153; b) R. D. Harcourt, *Nitric Oxide* **2017**, *69*, 51–55.
- [8] A. In-Iam, M. Wolf, C. Wilfer, D. Schaniel, T. Woike, P. Klüfers, *Chem. Eur. J.* **2019**, *25*, 1304–1325.
- [9] T. Schnepfensieper, S. Finkler, A. Czap, R. van Eldik, M. Heus, P. Nieuwenhuizen, C. Wreesmann, W. Abma, *Eur. J. Inorg. Chem.* **2001**, 491–501.
- [10] a) X. Wurzenberger, H. Piotrowski, P. Klüfers, *Angew. Chem. Int. Ed.* **2011**, *50*, 4974–4978; *Angew. Chem.* **2011**, *123*, 5078–5082; b) S. A. Cantalupo, S. R. Fiedler, M. P. Shores, A. L. Rheingold, L. H. Doerrer, *Angew. Chem. Int. Ed.* **2012**, *51*, 1000–1005; *Angew. Chem.* **2012**, *124*, 1024–1029; c) X. Wurzenberger, C. Neumann, P. Klüfers, *Angew. Chem. Int. Ed.* **2013**, *52*, 5159–5161; *Angew. Chem.* **2013**, *125*, 5264–5266.
- [11] G. Monsch, P. Klüfers, unpublished.
- [12] **1**-gallate: $\text{C}_{24}\text{H}_{30.67}\text{F}_{48}\text{FeGa}_2\text{NO}_{24.34}$, $M_r = 1829.83 \text{ g mol}^{-1}$, $0.10 \times 0.05 \times 0.02 \text{ mm}^3$, monoclinic, $P2_1/n$, $a = 19.5162(6) \text{ \AA}$, $b = 11.4432(3) \text{ \AA}$, $c = 25.1936(9) \text{ \AA}$, $\beta = 91.805(1)^\circ$, $V = 5623.6(3) \text{ \AA}^3$, $Z = 4$, $\rho_{\text{calc}} = 2.161 \text{ g cm}^{-3}$, $\mu = 1.442 \text{ mm}^{-1}$, MoK α , $\lambda = 0.71073 \text{ \AA}$, $T = 100(2) \text{ K}$, $2\theta_{\text{max}} = 52.8^\circ$, 51878 *hkl*, 11504 independent, $R_{\text{int}} = 0.0453$, $R = 0.0451$, $wR2 = 0.1190$, max. min^{-1} , residual $e\text{-density}$: 2.258/–1.140 $e \text{ \AA}^{-3}$. CCDC 1893483 contains the supplementary crystallographic data for this paper (1893482 for the **1**-ferrate). These data can be obtained free of charge from The Cambridge Crystallographic Data Centre.
- [13] a) S. Grimme, A. Hansen, *Angew. Chem. Int. Ed.* **2015**, *54*, 12308–12313; *Angew. Chem.* **2015**, *127*, 12483–12488; b) C. A. Bauer, A. Hansen, S. Grimme, *Chem. Eur. J.* **2017**, *23*, 6150–6164.
- [14] J. E. M. N. Klein, B. Miehl, M. S. Holzwarth, M. Bauer, M. Milek, M. M. Khusniyarov, G. Knizia, H.-J. Werner, B. Plietker, *Angew. Chem. Int. Ed.* **2014**, *53*, 1790–1794; *Angew. Chem.* **2014**, *126*, 1820–1824.
- [15] L. Freitag, S. Knecht, S. F. Keller, M. G. Delcey, F. Aquilante, T. Bondo Pedersen, R. Lindh, M. Reiher, L. Gonzalez, *Phys. Chem. Chem. Phys.* **2015**, *17*, 14383–14392.
- [16] a) M. Kaupp, *J. Comput. Chem.* **2007**, *28*, 320–325; b) H. S. Yu, S. L. Li, D. G. Truhlar, *J. Chem. Phys.* **2016**, *145*, 130901.
- [17] J. Cano, E. Ruiz, S. Alvarez, M. Verdaguier, *Comments Inorg. Chem.* **1998**, *20*, 27–56.
- [18] E. Ruiz, J. Cirera, S. Alvarez, *Coord. Chem. Rev.* **2005**, *249*, 2649–2660.
- [19] K. Boguslawski, C. R. Jacob, M. Reiher, *J. Chem. Theory Comput.* **2011**, *7*, 2740–2752.
- [20] P. Karen, P. McArdle, J. Takats, *Pure Appl. Chem.* **2016**, *88*, 831–839.
- [21] a) A. J. Webster, C. M. Mueller, N. P. Foegen, P. H. L. Sit, E. D. Speetzen, D. W. Cunningham, J. S. D’Acchioli, *Polyhedron* **2016**, *114*, 128–132; b) P. H. L. Sit, R. Car, M. H. Cohen, A. Selloni,

- Inorg. Chem.* **2011**, *50*, 10259–10267; c) A. J. W. Thom, E. J. Sundstrom, M. Head-Gordon, *Phys. Chem. Chem. Phys.* **2009**, *11*, 11297–11304; d) V. Postils, C. Delgado-Alonso, J. M. Luis, P. Salvador, *Angew. Chem. Int. Ed.* **2018**, *57*, 10525–10529; *Angew. Chem.* **2018**, *130*, 10685–10689; e) E. Ramos-Cordoba, V. Postils, P. Salvador, *J. Chem. Theory Comput.* **2015**, *11*, 1501–1508.
- [22] P. Salvador, unpublished.
- [23] A. Sadoc, R. Broer, C. de Graaf, *Chem. Phys. Lett.* **2008**, *454*, 196–200.
- [24] H. Hoshina, M. Slipchenko, K. Prozument, D. Verma, M. W. Schmidt, J. Ivanic, A. F. Vilesov, *J. Phys. Chem. A* **2016**, *120*, 527–534.
- [25] D. Beck, A. Belz, A. In-Iam, P. Mayer, P. Klüfers, *Z. Anorg. Allg. Chem.* **2017**, *643*, 1191–1194.

Manuscript received: March 13, 2019

Accepted manuscript online: April 24, 2019

Version of record online: May 17, 2019